RSC Advances

ROYAL SOCIETY OF CHEMISTRY

www.rsc.org/advances

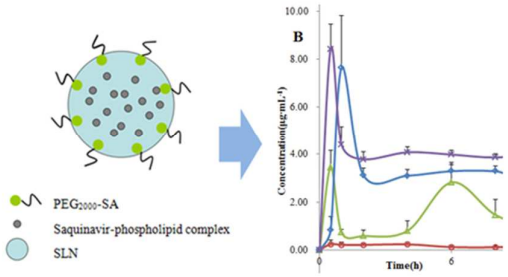

PEGylated solid lipid nanoparticles containing saquinavir indicated higher relative bioavailability which increased with enhancing the polyethylene glycol content in nanoparticles.

Journal Name

RSCPublishing

ARTICLE

Enhanced oral absorption of saquinavir mediated by PEGylated solid lipid nanoparticles†

Cite this: DOI: 10.1039/xoxxoooooox

Xiaoyu Hu[a], Xuqi Kang[b], Xiaoying Ying[b], Lejian Wang[b] and Yongzhong Du[b,*]

Received ooth January 2015,
Accepted ooth January 2015

DOI: 10.1039/xoxxoooooox

www.rsc.org/

PEGylated solid lipid nanoparticles containing saquinavir was prepared by solvent diffusion method combined with ionic complex, which indicated higher drug encapsulation efficiencies, drug loading capacity and slowed drug release behavior. Moreover, the nanoparticles presented low cytotoxicity, higher transport ability across intestinal epithelial cell, and hence higher relative bioavailability which increased with enhancing the polyethylene glycol content in nanoparticles.

1. Introduction

In recent years, human immunodeficiency virus (HIV) protease treatment of acquired immune deficiency syndrome (AIDS) has become an important potential target for antiretroviral therapy and remarkable progress has been made with respect to establish the HIV-encoded protease as viable target for chemotherapeutic intervention and toward developing potent inhibitors.[1] HIV protease inhibitors are a kind of drugs which were successfully designed based on the structure and reaction mechanism of the HIV protease,[2,3] therefore a variety of potent and specific inhibitors are listed now.

As the first HIV protease inhibitor which have been approved for marketing by the U.S. Food and Drug Administration (FDA) for the treatment of AIDS, saquinavir is a specific and high efficiency inhibitor of HIV-1 and HIV-2 proteinases *in vitro*[4] and shows bright prospects for developing and marketing.[5] But the deficiencies in metabolism, distribution, and oral bioavailability of these inhibitors, are still the chief remaining challenges. The saquinavir with poor oral bioavailability need a high dose regimen, which might increase the toxic and side effect. Therefore saquinavir needs to be further studied and discussed about how to improve the oral bioavailability and transform it as an effective therapeutic agent for the market.

Recently, nanocarriers, due to their small size and target specific localization properties, are being actively investigated, and higher bioavailability and increased residence time of the drugs can be achieved. For instance, solid lipid nanoparticles (SLNs) have been focused on as a new developed type of colloidal drug delivery systems,[6] which can replace fat emulsions,[7] liposomes[8] and polymeric nanoparticles[9] The particle size of these solid colloidal particles ranges from 10 to 1,000 nm and natural or synthetic solid lipid can be used as a carrier[10,11] wherein the drug is surrounded or dispersed and then a solid particles structural system was formed. As a drug carrier, SLNs integrate the advantages of drug-containing microemulsions and liposomes, and can improve the bioavailability of drugs, physiological compatibility.[12-14] The pharmacokinetics of a drug can be changed greatly when the drug is packaged into nanoparticles, owing to the controlled release of the drug from the nanoparticles and the alteration in body distribution of the drug.[15] In brief, SLNs could effectively enhance the oral absorption and bioavailability as an oral drug carrier while reducing the dose to lower the toxic and side-effect. However, the SLNs had some disadvantages such as low drug loading capacity which usually as low as 5%, and low drug encapsulation efficiency.[15-17]

Phospholipids complex has been studied for many years to improve the drug loading capacity and enhance the therapeutic efficacy of some drugs with poor oral absorption.[18,19] In this research, saquinavir was firstly complex with phospholipid by ionic interaction for improving drug loading capacity based on the compatibility between phospholipid and lipid matrix. Then the solid lipid nanoparticles containing saquinavir[20] (SQV-SLNs) were prepared by solvent diffusion method to enhance the oral absorption and bioavailability of the drug, and the effect of polyethylene glycol (PEG) modification on the physiochemical properties of nanoparticles including particle size, cellular uptake and transport ability across intestinal epithelial cell monolayer, *in vivo* residence time and relative bioavailability were investigated in details.

2. Materials and methods

2.1. Materials.

Monostearin was purchased from Chemical Reagent Co., Ltd. (Shanghai, China). Polyethylene glycol monostearate (PEG_{2000}-SA, M_w=2000) was supplied by Tci Development Co., Ltd. (Shanghai, China). Phospholipid (Lipoid®S 100; soybean lecithin) was supplied by Lipoid GmbH (Ludwigshafen,-Germany). Octadecylamine (ODA) was purchased from Fluka, U.S.A. Hoechst 33342 and fluorescein isothiocyanate (FITC) were obtained from Sigma-Aldrich (St. Louis, MO, U.S.A.). MDCK cell lines were obtained from the Institute of Biochemistry and Cell Biology (Shanghai, China). Fetal bovine serum (FBS) was purchased from Gibco (Grand Island, NY, U.S.A.). Dulbecco's modified Eagle's medium (DMEM, 4.5 g/L glucose) culture solution, trypsin and ethylene diamine tetraacetic acid (EDTA) were purchased from Gibco BRL (U.S.A.). N-2-Hydroxyethylpiperazine-N-2-ethanesulfonic acid (HEPES) was purchased from Sigma Saint Quentin Fallavier

(France). All other chemical reagents were analytical grade or better.

SD rats were purchased from shanghai laboratory animal center. The animal studies were approved by the Ethical Committee of Zhejiang University, Hangzhou, China.

2.2. Preparation and characterization of saquinavir-phospholipids complex.

For prepare saquinavir-phospholipid ionic complex, 10 mg saquinavir and 15 mg phospholipids were weighted and placed in a round-bottom flask and dissolved in 2 mL anhydrous ethanol. After ethanol was completely evaporated under vacuum at 50 °C, a uniform and transparent film was formed. The differential scanning calorimetry (DSC) curve of resultant saquinavir-phospholipid complex was performed by using Differential Scanning Calorimeter (DSC Q200, Universal V3.8A TA Instruments, USA).

2.3. Preparation and characterization of SLNs and pSLNs.

The solid lipid nanoparticles loading saquinavir (SQV-SLNs) were then prepared by solvent diffusion method in an aqueous system. 25 mg saquinavir-phospholipid ionic complex was dissolved in 1 mL ethanol, and 25 mg monostearin was then dissolved in this solution in water bath at 50 °C. The resultant organic solution was quickly dispersed into 9 mL distilled water under mechanical agitate in water bath at 50 °C for 5 min. The obtained pre-emulsion was allowed to cool at room temperature, until solid lipid nanoparticles loading saquinavir dispersion was obtained. For preparation of PEGylated solid lipid nanoparticles loading saquinavir (pSLNs), 5, 10 wt% PEG_{2000}-SA relating to the mass of SQV-SLNs was used instead for the mass of monostearin. The SQV-SLNs containing 0%, 5% and 10% PEG_{2000}-SA was termed as SLNs, pSLNs-5% and pSLNs-10%, respectively.

After the SQV-SLNs were prepared, the number average diameter of obtained SQV-SLNs and pSLNs in suspension was determined with Zetasizer (3000HS, Malvern Instruments Ltd., UK) after the suspension diluted 50 times with distilled water. The morphologies of SQV-SLNs and pSLNs were also observed by transmission electron microscopy (TEM) (JEM-1200EX, JEOL, Japan). The samples were diluted 100 times and placed on copper grids with films and then stained with 2% (w/v) phosphotungstic acid for viewing by TEM.

Drug encapsulation efficiency (EE%) and drug loading capacity (DL%) should be determined. The entrapment efficiency was determined by measuring the content of free drug in the dispersion medium. And the High Performance Liquid Chromatography (HPLC) was mainly used to determine the content of saquinavir. The saquinavir content diluted in mobile phase (C_1, μg/mL) was determined. The entrapment efficiency (EE, %) and drug loading (DL, %) of saquinavir in the SQV-SLNs were then calculated from eqs 1 and 2, respectively.

$$EE=\frac{W_a-C_1\times V}{W_a}\times 100\% \quad (1)$$

$$DL=\frac{W_a-C_1\times V}{W_a-C_1\times V+W_b+W_0}\times 100\% \quad (2)$$

where W_a, W_b and W_0 denoted the charged amount of saquinavir (mg) , monostearin and PEG_{2000}-SA (mg) and weight of lipid (mg) added in the system, and V represented the total volume of mobile phase solution (mL).

In vitro drug release from SLNs was further measured by the dialysis bag method.[21] 1 mL of the original precipitate of SLNs in preparation was loaded into dialysis membrane (MWCO: 14.0 kDa, Spectrum Laboratories, Laguna Hills, CA) and added in a 50 mL plastic tube containing 15 mL release medium (phosphate buffer, pH 7.4). The drug content was analyzed by HPLC method as described above. Using saquinavir solution as a control, the release profiles of SLNs, pSLNs-5% and pSLNs-10% were performed.

2.4. Pharmacokinetic studies.

The pharmacokinetic study was then performed using male SD rats (230 ± 10 g, Laboratory Animal Center, Zhejiang University, China). The rats were fasted 12 h before experiment but had free access to water and were divided at random into four sets (five rats per set). The first group received saquinavir suspension (54 mg/kg) by oral gavage. The other groups received SLNs, pSLNs-5% and pSLNs-10% (54 mg/kg) by oral gavage. After administration, 0.5 mL blood samples were withdrawn from the tail vein into a heparin-rinsed vial at different time intervals. The whole blood samples were centrifuged at 5000 rpm for 10 min to obtain serum which was frozen at -20 °C until analysis. Then, saquinavir concentrations in these samples were measured.

Saquinavir content was determined by HPLC method. For analysis, the serum sample (80 μL) was vortex-mixed with 40 μL potassium dihydrogen phosphate solution (0.01 mol/L, pH 7.5) and 1 mL ether for 2 min. This mixture was extracted using 4 mL of ethyl ether with shaking for 20 min. The solution was centrifuged at 8,000 rpm for 10 min, and the supernatant was evaporated. The residue in the tube was added to 100 μL of the mobile phase for the HPLC analysis.

2.5. Permeation tests across MDCK cell monolayer.

The transport experiments of SLNs and pSLNs were conducted using Madin-Daby canine kidney (MDCK) cell as a model intestinal epithelial cell line. The cytoxicity of SLNs and pSLNs against MDCK cells were performed by MTT assay. Briefly, 1×10^4 cells/well were seeded in a 96-well plate (Nalge Nunc International, Naperville, IL, USA) and treated with serial concentrations of SLNs and pSLNs (125−625 μg/mL), cells were incubated for further 48 hours, and then MTT was added. After removing the unreduced MTT and medium, Dimethyl sulfoxide (DMSO) were added to dissolve the formazan crystals with 30 min of shaking before absorption was measured.

The permeation tests of SLNs and pSLNs were conducted using MDCK cell monolayers. Before and after the experiment, the integrity of the monolayers was assessed by measuring the transepithelial electrical resistance (TEER) values using a Millicell-ERS volt-ohmmeter (Millipore Co., USA). For permeation test, 0.5 mL transport medium containing nanoparticles (20 μg/mL of saquinavir equivalent) was applied to the apical side followed by addition of 1.5 mL blank transport medium to the basolateral side. At certain time intervals, the transport medium in basolateral side was collected and rapidly replaced with equivalent fresh transport medium. The content of saquinavir was detected by HPLC. And the apparent permeability coefficient (P_{app}) was calculated from the measurement of the transfer rate of saquinavir across MDCK cells from upper to lower compartments of the transwell diffusion cells.

2.6. Cellular uptake investigation.

The cellular uptake assay of SLNs, pSLNs-5% and pSLNs-10% were performed using MDCK cells as model cells. For this assay, the nanoparticles were fluorescence labeled by

the chemical conjugate of otcadecylamine and fluorescein isothiocyanate (ODA-FITC). After the MDCK cells were incubated with SLNs, pSLNs-5% and pSLNs-10% for 1, 2 and 8 h, the cells were washed with PBS and observed using an inverted fluorescence microscope (Nikon Eclipse Ti; Technical Instruments, San Francisco, CA).

3. Results and discussion

3.1. Preparation and characterization of saquinavir-phospholipids complex.

Saquinavir-phospholipids complex was prepared by the ionic interaction between saquinavir and phospholipids. The DSC curve of resultant saquinavir-phospholipid complex was performed by using DSC. Fig. 1 showed the DSC curves of saquinavir, phospholipids, physical mixture of saquinavir and phospholipids, and saquinavir-phospholipids ionic complex. No endothermic peak around 120 °C was found from the thermogram of saquinavir-phospholipids ionic complex, which was observed in the curves of physical mixture of saquinavir and phospholipids. The melting peak around 74 °C of saquinavir-phospholipids ionic complex was found wider than that in the thermogram of physical mixture of saquinavir and phospholipids, and the phase transition temperature of saquinavir-phospholipids ionic complex was lower than the phase transition temperature of physical mixture of saquinavir and phospholipids. The results were considered that ionic bonds were formed between the amino group of saquinavir and the phosphate group of phospholipids, in other words, saquinavir-phospholipids ionic complex was formed.

3.2. Preparation and characterization of SLNs and pSLNs.

The solid lipid nanoparticles containing saquinavir was then prepared by solvent diffusion method using saquinavir-phospholipids ionic complex. Physiochemical properties of SQV-SLNs including particle size, morphology, drug encapsulation efficiency (EE%) and drug loading capacity (DL%), *in vitro* release characteristics were measured and

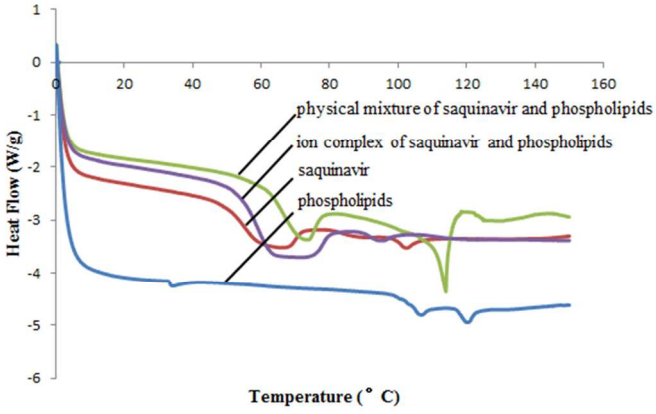

Fig. 1 DSC curves of saquinavir, phospholipids, physical mixture of phospholipids and saquinavir, and saquinavir-phospholipid ionic complex.

Table 1 Physicochemical properties of prepared SQV-SLNs containing different amount of PEG_{2000}-SA.

PEG_{2000}-SA Content (wt%)	Size (nm)	PI	EE (%)*	DL (%)*
0	275±34.90	0.509	99.19±0.01	19.87±0.01
5	220±22.45	0.443	98.40±0.15	19.74±0.02
10	158±15.95	0.449	95.23±0.13	19.23±0.02

*Each value represented the mean ± SD (n = 3)

evaluated. The size measurement results were shown in Table 1. The results indicated that the number average diameter of SQV-SLNs was about 275 nm, and the incorporation of PEG_{2000}-SA led to the formation of spherical nanoparticles with smaller particle size. The number average diameter of pSLNs-10% was about 158 nm. The TEM images of SLNs and pSLNs were presented in Fig. 2. The photographs revealed that all of nanoparticles for SQV-SLNs, pSLNs-5% and pSLNs-10% had spherical shapes, and the size of the nanoparticles shown in the Fig. 2 determined by the TEM were found smaller than the size determined by the Zetasizer which could be illustrated by the theory that the nanoparticles were in an expanded state in solution when the size were determined by the Zetasizer while the particles would be dried when the TEM photographs were taken. In this case, the results that the size of the nanoparticles reduced with increasing the content of PEG_{2000}-SA in nanoparticles could be revealed by the results of the TEM which were accordance to that of Zetasizer determination.

Table 1 also indicated the drug encapsulation efficiencies (EE%) and drug loading capacities (DL%) of prepared SQV-SLNs containing different amount of PEG_{2000}-SA. The higher drug encapsulation efficiencies were obtained, saquinavir using the preparation method combined ionic complex with solvent diffusion method, which were above 95 %. SQV-SLNs had the highest drug encapsulation efficiency which was about 99.19 %, and the drug encapsulation efficiency slightly decreased with increasing the content of PEG_{2000}-SA. The drug encapsulation efficiency of pSLNs-10% was about 95.23 %, which were much higher than that of conventional SLNs.[16,17] Usually, the drug loading capacity of SLNs was lower than 5%. The formation of saquinavir-phospholipid ionic complex could enhance the compatibility between saquinavir and lipid matrix. As a result, the drug encapsulation efficiency and loading capacity were highly improved.

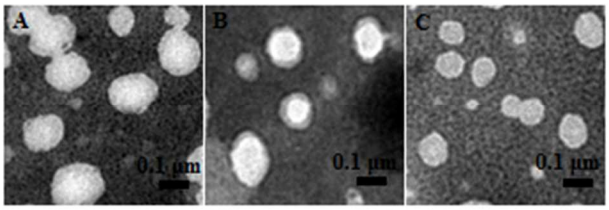

Fig. 2 TEM photographs of SQV-SLNs with 0% PEG_{2000}-SA content (A); pSLNs-5% (B); pSLNs-10% (C), scale bar = 0.1 μm.

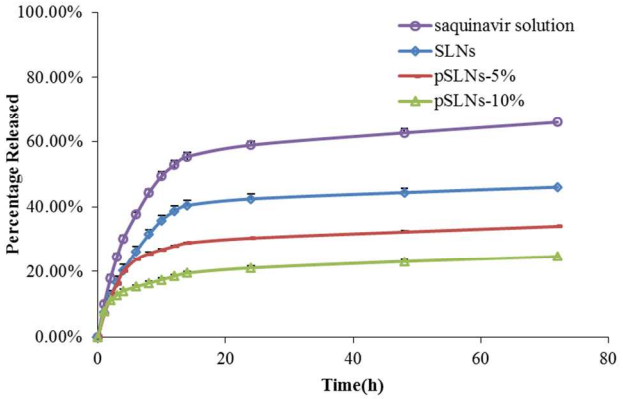

Fig. 3 *In vitro* saquinavir release profiles of SLNs, pSLNs-5% and pSLNs-10%, using saquinavir solution as a control. (n = 3).

In vitro drug release from SLNs was further measured by the dialysis bag method. Using saquinavir solution as a control, the release profiles of SQV-SLNs, pSLNs-5% and pSLNs-10% were showed in Fig. 3. It was obvious that saquinavir release behaviours from SLNs, pSLNs-5% and pSLNs-10% were slower than that of the diffusion for saquinavir solution from the dialysis bag. A biphasic drug release pattern were found in SLNs, pSLNs-5% and pSLNs-10%, which presented burst drug release at the initial stage and subsequently sustained release at the latter stage. The initial burst drug release might originate from the saquinavir adsorbed on the surface of nanoparticles or near the surface of nanoparticles. On the other hand, the PEG_{2000}-SA modification of the SQV-SLNs could decelerate release of saquinavir from SQV-SLNs in the initial stage, and no effect to the drug release rate was observed in the latter stage. In the initial stage, the released drugs were the drug located near the surface of nanoparticles. The PEG_{2000}-SA modification could cause a sterical hindering effect and the most structured interfacial membrane which could restrict saquinavir transport and slow down the degradation.[22,23] In the latter stage, the released drugs were the drug loaded in the core of nanoparticles, which were released based on the corrosion of lipid matrix in SLNs, and no effect was observed for incorporation of PEG_{2000}-SA in SLNs.

3.3. Pharmacokinetic Studies.

To further investigate the *in vivo* behavior of solid lipid nanoparticles loading saquinavir, the pharmacological effects of SQV-SLNs were evaluated on male SD rats. The curves of plasma concentration of saquinavir after a single oral dose (54 mg/kg) were illustrated in Fig 4. It was found the plasma concentration and residence time of SLNs, pSLNs-5% and pSLNs-10% were improved than that of saquinavir suspension, and which enhanced with the PEG_{2000}-SA content in SLNs. Interestingly, the rats receiving SLNs, pSLNs-5% and pSLNs-10% exhibited a concentration-time profile characterized by an early peak followed by a smaller peak and a continuous decay in the plasma concentration, indicating a bimodal distribution. However, the rats receiving saquinavir suspension only showed an early peak. These results indicated that SLNs were transported across the gastrointestinal tract into systematic circulation quickly, but also presented a hepatoenteral circulation.[24]

Pharmacokinetic parameter calculations were then performed on each individual set of data, and the pharmacokinetic software DAS version 2.0.1 (Mathematical Pharmacology, Professional Committee of China, Shanghai, People's Republic of China) was used to calculate the standard non-compartmental pharmacokinetic parameters (± SD). The key pharmacokinetic parameters obtained by a noncompartmental analysis after the oral administration of saquinavir suspension, SLNs, pSLNs-5% and pSLNs-10% were given in Table 2. It was obvious that the C_{max} (peak plasma saquinavir concentration) and MRT (the mean residence time) were highly improved when the drug was encapsulated into SLNs, and which were significantly enhanced with increasing the PEG_{2000}-SA content in SLNs. Comparing with saquinavir suspension, the C_{max} of pSLNs-10% was increased 24.52-fold, and the MRT_{0-t} increased from 4.62 h to 51.68 h. The AUC and relative bioavailability of saquinavir was enhanced near 1-fold, however, which were highly improved by the PEGylation of SLNs. The relative bioavailability of saquinavir for pSLNs-10% was 101.15-fold higher than that of saquinavir suspension. The improved transport efficiency across the gastrointestinal tract and prolonged blood circulation times contributed by the higher PEG_{2000}-SA content led to the longer residence time and the higher AUC and relative bioavailability.[25]

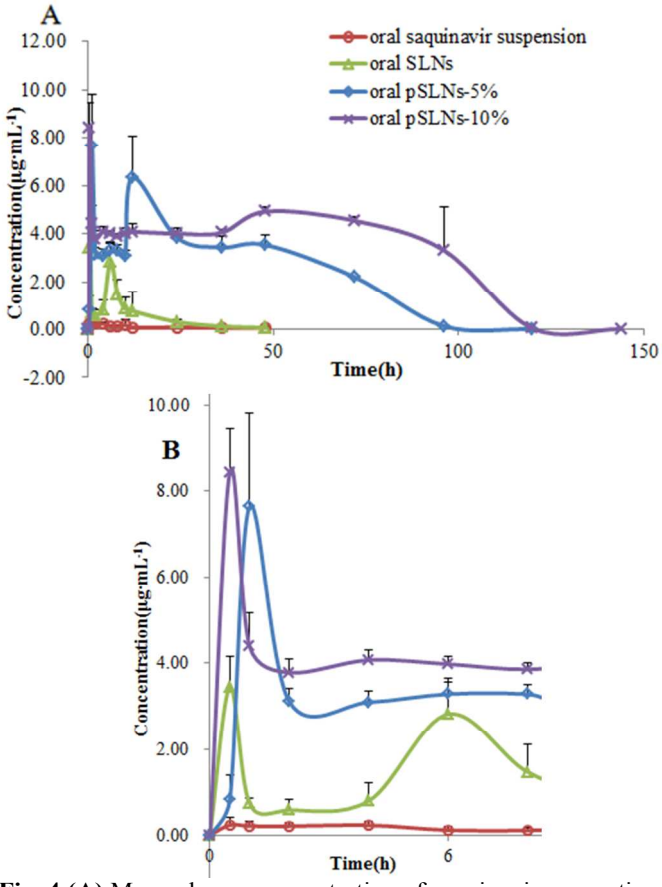

Fig. 4 (A) Mean plasma concentration of saquinavir versus time curves after oral administration of saquinavir to rats at a dose of 54 mg/kg from saquinavir suspension, SLNs, pSLNs-5% and pSLNs-10%. Each value represented the mean ± SD (n = 5). **(B)** Enlarged figure of mean plasma concentration of saquinavir versus time curves.

Table 2. Pharmacokinetic parameters[a] of saquinavir formulations (dose 54 mg/kg) after oral administration of saquinavir suspension, SLNs, pSLNs-5% and pSLNs-10% to Rats*

PK	control	SQV-SLNs		
		SLNs	pSLNs-5%	pSLNs-10%
AUC_{0-t} (mg/L·h)	4.43	8.89	273.59	448.11
MRT_{0-t} (h)	4.62	11.88	36.21	51.68
C_{max}(mg/L)	0.33	3.58	7.46	8.42
T_{max}(h)	3.80	1.88	0.5	0.50
K_e(1/h)	0.06	0.08	0.02	0.01
relative bioavailability	100%	200.68%	6175.85%	10115.35%

*Each value represented the mean ± SD (n = 5)

[a]PK: pharmacokinetics parameters. T_{max}: the time when peak plasma saquinavir concentration was reached. C_{max}: peak plasma saquinavir concentration. MRT: the mean residence time. K_e: the elimination rate constant of saquinavir in the systemic circulation. AUC_{0-t}: area under the plasma saquinavir concentration time curve.

3.4. Permeation tests across MDCK cell monolayer..

The cytoxicity of SLNs and pSLNs against MDCK cells were performed by MTT assay firstly. Fig. 5 showed the cytotoxicity of blank and saquinavir-loaded nanoparticles. The cell viabilities after incubation with blank nanoparticles for 48h at the tested concentration were around 100%, which showed that the lipid materix had no obvious cytotoxicity and were appropriate for using as oral drug carriers. After drug loading, the nanoparticles indicated slight cytotoxicity, and the pSLNs showed less toxicity than SLNs. The 50% inhibition concentration (IC_{50}) of SLNs could be calculated at 269.02 μg/mL, while the IC_{50} of pSLNs-5% and pSLNs-10% were 549.25 μg/mL and 550.47 μg/mL, respectively. The cytotoxicity was decreased with the increasing the ratio of PEG in SLNs. These results demonstrated that SLNs and pSLNs had low cytotoxicity, and the cell survival rate was approximately 100% when the concentration of SLNs was 100 μg/mL, which were used for further experiments.

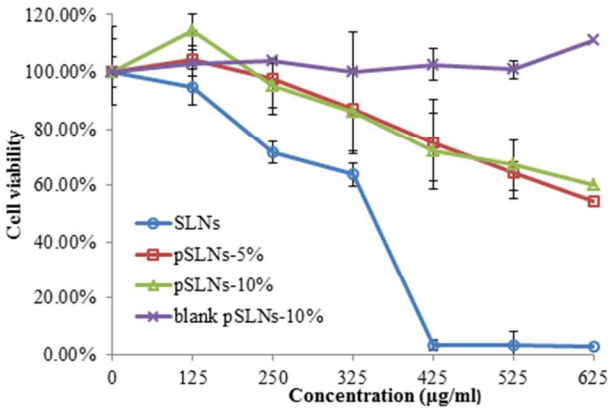

Fig. 5 Cytotoxic effect of SLNs and pSLNs incubated with MDCK cells. Each value represented the mean ± SD (n = 3).

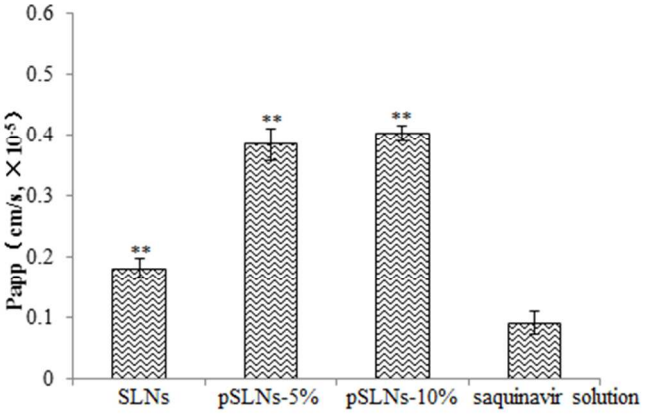

Fig. 6 The apparent permeability coefficient (P_{app}) of SLNs, pSLNs-5%, pSLNs-10% and saquinavir solution across MDCK cell monolayers (n = 3). $^{**}p < 0.01$ compared with saquinavir solution.

To investigate the transport efficacy of the nanoparticle across intestinal epithelial cell, the permeation properties of drug-loaded SLNs were evaluated by comparing SQV-SLNs, pSLNs-5% and pSLNs-10% with saquinavir solution in MDCK cell monolayers. The cell monolayers with TEER values above 180 Ω·cm^2 were selected for the subsequent studies.[26] Before and after the experiment was performed, the integrity of the cell monolayers was assessed by measuring the TEER values. The TEER values before and after the experiment were around 250Ω·cm^2 which indicated the monolayer was integrated and the results of the transport experiments were reliable. As shown in Fig. 6, comparing with saquinavir solution, the P_{app} value of SLNs pSLNs-5% and pSLNs-10% were gradually increased. All of SLNs, pSLNs-5% and pSLNs-10% showed significantly higher drug permeation compared with saquinavir solution. Furthermore, the drug transport ability across intestinal epithelial cell monolayer enhanced with increasing the PEG_{2000}-SA content in SLNs. Numerous studies highlighted the potential of nanoparticles in improving the gastrointestinal absorption and oral bioavailability *in vivo*.[9,27] It was also reported that the PEGylation of nanoparticles could significantly enhance the ability to convert nanoparticles from mucoadhesive to mucoinert.[28,29]

3.5. Cellular Uptake Investigation

To explore the enhanced transport mechanism of SLNs and pSLNs across intestinal epithelial cell monolayer, the cellular uptake assay of SQV-SLNs, pSLNs-5% and pSLNs-10% were performed using MDCK cells as model cells to explore the enhanced transport mechanism of SLNs and pSLNs across intestinal epithelial cell monolayer. As shown in Fig. 7, the cellular uptake of the nanoparticles was time dependent, and the pSLNs had faster cellular uptake ability. The cellular uptake ability was increased with the increasing ratio of PEG possibly because the pSLNs had the smaller size. It has been proven that a small particle size contributed to endocytosis.[30] And the results also demonstrated that the transport ability across intestinal epithelial cell monolayer of nanoparticles increased by increasing the amount of PEG fraction on nanoparticles surface, which could improve the hydrophilicity of SLNs.[31]

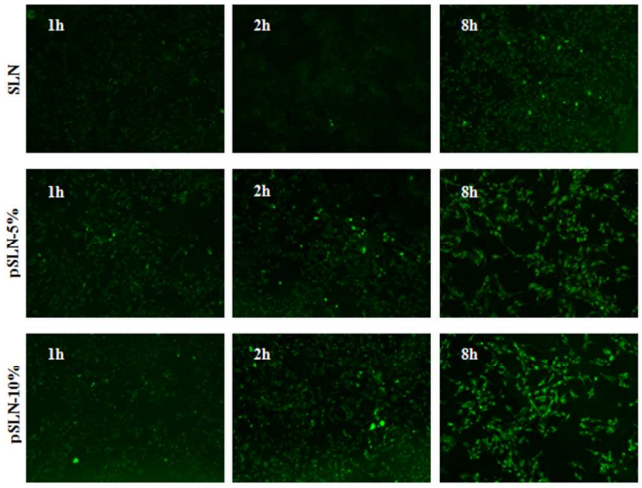

Fig. 7 Fluorescence images of MDCK cells incubated with SLNs, pSLNs-5% and pSLNs-10% (drug content was 20 μg/mL) for 1 h, 2 h and 8 h.

Conclusions

The solid lipid nanoparticles loading saquinavir were successfully prepared using the combination of ionic complex and solvent diffusion method in an aqueous system, which had high drug encapsulation efficiencies and drug loading capacities. The higher PEG_{2000}-SA content in SLNs led to smaller particle size, slower drug release behavior in initial stage, stronger cellular uptake and transport ability across intestinal epithelial cell monolayer, longer *in vivo* residence time, and higher relative bioavailability. These properties suggested that PEGylated solid lipid nanoparticles loading saquinavir was a new promising oral anti-HIV drug delivery system.

Acknowledgements

We are grateful for financial support from the technology and social development project of Ningbo Science and Technology Bureau under contract 2010C50035 and Medical and health research funding schemes of Zhejiang Province under contract 2012KYA064.

Notes and references

[a] Zhejiang Pharmaceutical College, Ningbo 315100, China
[b] College of Pharmaceutical Sciences, Zhejiang University, 866 Yuhangtang Road, Hangzhou 310058, China, E-mail: duyongzhong@zju.edu.cn; Fax: +86-0571-88208439; Tel: +86-0571-88208439
† Electronic Supplementary Information (ESI) available. See DOI: 10.1039/b000000x/

1 Huff J R., *J Med Chem.*, 1991, **34**, 2305.
2 Wlodawer A1, Vondrasek J., *Annu Rev Biophys Biomol Struct.*, 1998, **27**, 249.
3 Kim RB, Fromm MF, Wandel C, Leake B, Wood AJ, Roden DM, Wilkinson GR, *J Clin Invest.*, 1998, **101**, 289.
4 Evan T. Brower, Usman M. Bacha, Yuko Kawasaki and Ernesto Freire, *Chem Biol Drug Des.*, 2008, **71**, 298.
5 Rossignol JF., *Exp Parasitol*., 2010, **124**, 45.
6 Almeida and Eliana Souto, *Adv Drug Deliv Rev.*, 2007, **59**, 478.
7 Frederike Tenambergen, Cintia H. Maruiama1 and Karsten Mäder, *Int J Pharm.*, 2013, **447**, 31.
8 Qiyu Huang, Lili Zhang, Xiaoyi Sun, Ke Zeng, Juan Li and You-Nian Liu, *RSC Adv.*, 2014, **4**, 59211.
9 Laura M. Ensign, Richard Cone and Justin Hanes, *Adv Drug Deliv Rev.*, 2012, **64**, 557.
10 Suphiya Parveen, Ranjita Misra and Sanjeeb K. Sahoo, *Nanomedicine: Nanotechnology, Biology and Medicine*, 2012, **8**, 147.
11 Surajit Das, Wai Kiong Ng and Reginald B.H. Tan, *Eur J Pharm Sci.*, 2012, **47**, 139.
12 Mei L, Zhang Z, Zhao L, Huang L, Yang XL, Tang J, Feng SS., *Adv Drug Deliv Rev.*, 2013, **65**, 880.
13 Gastaldi L, Battaglia L, Peira E, Chirio D, Muntoni E, Solazzi I, Gallarate M, Dosio F, *J Pharm Biopharm.*, 2014, **87**, 433.
14 Almeida, H., Amaral, M. H., Lobão, P., Silva, A. C., & Loboa, J. M. S., *J Pharm Pharm Sci.*, 2014, **17**, 278.
15 Müller RH, Mäder K, Gohla S., Eur *J Pharm Biopharm*., 2000, **50**, 161.
16 Blasi P, Giovagnoli S, Schoubben A, Ricci M, Rossi C., *Adv Drug Deliv Rev.*, 2007, **59**, 454.
17 Müller RH, Radtke M, Wissing SA, *Adv Drug Deliv Rev.*, 2002, **54**, 131.
18 Zhao YQ, Wang LP, Ma C, Zhao K, Liu Y, Feng NP. *Int J Nanomedicine.*, 2013, **8**, 4169.
19 Jin X, Zhang ZH, Sun E, Tan XB, Zhu FX, Jia XB. *Drug Dev Ind Pharm.*, 2013, **39**, 1421.
20 Dodiya SS, Chavhan SS, Sawant KK, Korde AG., *J Microencapsul.*, 2011, **28**, 515.
21 Hu FQ, Liu LN, Du YZ, Yuan H., *Biomaterials.*, 2009, **30**, 6955.
22 Silvander M, Hansson P, Edwards K., *Langmuir*, 2000, **16**, 3696.
23 Su Z, Niu J, Xiao Y, Ping Q, Sun M, Huang A, You W, Sang X, Yuan D., *Mol Pharm.*, 2011, **8**, 1641.
24 Zhu H, Zhang X, Guan J, Cui B, Zhao L, Zhao X., *J Pharm Biomed Anal.*, 2013, **78-79**, 136.
25 Yuan H, Chen CY, Chai GH, Du YZ, Hu FQ., *Mol Pharm.*, 2013, **10**, 1865.
26 Chai GH, Hu FQ, Sun J, Du YZ, You J, Yuan H., *Mol Pharm.*, 2014, **11**, 3716.
27 Ji H, Tang J, Li M, Ren J, Zheng N, Wu L., *Drug Deliv.*, 2014, **3**, 1.
28 Yuan H, Chen CY, Chai GH, Du YZ, Hu FQ., *Mol Pharm.*, 2013, **10**, 1865.
29 Wang YY, Lai SK, Suk JS, Pace A, Cone R, Hanes J., *Angew. Chem. Int. Ed. Engl.*, 2008, **47**, 9726.
30 Decuzzi P, Ferrari M., *Biophys J.*, 2008, **94**, 3790
31 Cavalli R, Caputo O, Gasco MR., *Eur J Pharm Sci.*, 2000, **10**, 305.

